Journal of Antimicrobial Chemotherapy (2009) **63**, 1163–1172
doi:10.1093/jac/dkp129
Advance Access publication 17 April 2009

JAC

Assessment of methylthioadenosine/*S*-adenosylhomocysteine nucleosidases of *Borrelia burgdorferi* as targets for novel antimicrobials using a novel high-throughput method

Kenneth A. Cornell[1], Shekerah Primus[2], Jorge A. Martinez[1] and Nikhat Parveen[2]*

[1]Department of Chemistry and Biochemistry, Boise State University, 1910 University Drive, Boise, IA 83725-1520, USA; [2]Department of Microbiology and Molecular Genetics, University of Medicine and Dentistry of New Jersey, New Jersey Medical School, 225 Warren Street, Newark, NJ 07103-3535, USA

Received 4 February 2009; returned 3 March 2009; revised 10 March 2009; accepted 12 March 2009

***Background*: Lyme disease is the most prevalent tick-borne disease in the USA with the highest number of cases (27 444 patients) reported by CDC in the year 2007, representing an unprecedented 37% increase from the previous year. The haematogenous spread of *Borrelia burgdorferi* to various tissues results in multisystemic disease affecting the heart, joints, skin, musculoskeletal and nervous system of the patients.**

***Objectives*: Although Lyme disease can be effectively treated with doxycycline, amoxicillin and cefuroxime axetil, discovery of novel drugs will benefit the patients intolerant to these drugs and potentially those suffering from chronic Lyme disease that is refractory to these agents and to macrolides. In this study, we have explored 5′-methylthioadenosine/*S*-adenosylhomocysteine nucleosidase as a drug target for *B. burgdorferi*, which uniquely possesses three genes expressing homologous enzymes with two of these proteins apparently exported.**

***Methods*: The recombinant *B. burgdorferi* Bgp and Pfs proteins were first used for the kinetic analysis of enzymatic activity with both substrates and with four inhibitors. We then determined the antispirochaetal activity of these compounds using a novel technique. The method involved detection of the live–dead *B. burgdorferi* by fluorometric analysis after staining with a fluorescent nucleic acids stain mixture containing Hoechst 33342 and Sytox Green.**

***Results*: Our results indicate that this method can be used for high-throughput screening of novel antimicrobials against bacteria. The inhibitors formycin A and 5′-*p*-nitrophenythioadenosine particularly affected *B. burgdorferi* adversely on prolonged treatment.**

***Conclusions*: On the basis of our analysis, we expect that structure-based modification of the inhibitors can be employed to develop highly effective novel antibiotics against Lyme spirochaetes.**

Keywords: Lyme disease, enzyme inhibitors, Bgp, fluorometric assay, spirochete

Introduction

Lyme disease, caused by the spirochaete *Borrelia burgdorferi*, is the most prevalent tick-borne multisystemic illness and affects the heart, joints, skin, musculoskeletal and nervous system. Persistent infection with the spirochaete results in potentially incapacitating arthritis, neuroborreliosis, acrodermatitis chronicum atrophicans and carditis. Doxycycline, amoxicillin or cefuroxime axetil are recommended as the first-line therapy for early and late Lyme disease. Macrolides are less effective against *B. burgdorferi*,[1,2] and resistance of these spirochaetes to erythromycin has been reported.[3] As a result, macrolides, including azithromycin, clarithromycin and erythromycin, are recommended only for patients intolerant to the first-line therapy. Hence, discovery of new antimicrobials that could be used alone or in combination with other antibiotics will be highly beneficial for drug-intolerant patients and potentially for patients suffering from chronic Lyme disease that is refractory to other agents.

One potential drug target that has been identified is the enzyme 5′-methylthioadenosine/*S*-adenosylhomocysteine

*Corresponding author. Tel: +1-973-972-4483 ext. 25218; Fax: +1-973-972-8981; E-mail: Parveeni@umdnj.edu

(MTA/SAH) nucleosidase,[4] an enzyme present in most bacterial species but absent in humans. MTA/SAH nucleosidase cleaves the glycosidic linkage of the nucleosides to generate the thiosugars 5-methylthioribose (MTR) or *S*-ribosylhomocysteine (SRH) and the purine adenine.[5] In bacteria, MTA is produced from *S*-adenosylmethionine (SAM) as a by-product of polyamine, autoinducer I and biotin synthesis, while SAH is derived from SAM-mediated methylation reactions. MTR and SRH can be salvaged through separate routes to methionine, while adenine re-enters the purine pools of the cell. Cleavage of SRH by the enzyme LuxS yields homocysteine, which can be remethylated to methionine, and 4,5-dihydroxy-2,3-pentanedione (DPD), a precursor for autoinducer-2 (AI-2) synthesis. Thus, the activity of the nucleosidase is connected to the production of two bacterial quorum-sensing autoinducers.[6–8] These autoinducers are involved in the induction of various virulence factors in bacteria and contribute to their pathogenesis.[6–8]

Nucleosidase inhibitors could exert antimicrobial actions by one or more mechanisms and have been explored as a target for the design of the broad-spectrum antibiotics against Gram-positive and Gram-negative bacteria by several laboratories.[4,9–15] MTA and SAH are known to inhibit polyamine synthase[16,17] and methyltransferase[18] activities in various organisms. Thus, inhibition of the nucleosidase could work by promoting a build-up of MTA and SAH to growth-inhibitory levels. In addition, the loss of salvage of purine and methionine components may suppress bacterial growth by nutrient limitation, and because it is energetically expensive to make methionine *de novo*.

Due to the absence of major biosynthetic pathways, it is particularly important for the nutritional auxotroph, *B. burgdorferi*, to recycle metabolic by-products. However, *Borrelia* species lack methionine synthase (*metH*), which is required to remethylate homocysteine to methionine, and do not have a functional *mtnK* gene (methylthioribose kinase) required to salvage methionine from MTR.[19] Loss of adenine salvage by nucleosidase inhibition may have a significant effect on *B. burgdorferi*, since they are purine auxotrophs. Alternatively, interruption of the synthesis of SRH and DPD, and subsequent loss of AI-2 signalling may represent a unique aspect of nucleosidase inhibitors[7,20] as Lyme spirochaetes are known to synthesize AI-2 and alter surface protein expression in response to this autoinducer.[21,22]

Previously, we identified a glycosaminoglycan-binding protein located on the surface of *B. burgdorferi* and named it *Borrelia* glycosaminoglycan-binding protein or Bgp.[23] Interestingly, Bgp is homologous to the cytoplasmic Pfs protein present in a wide variety of bacterial species and also exhibits MTA/SAH nucleosidase activity.[24] The genome sequence of *B. burgdorferi* shows the presence of three Pfs homologues: Pfs (BB0375), Bgp (BB0588) and MtnN (BBI06).[25] The translated sequences for *bgp* and plasmid-borne *mtnN* genes contain predictable signal peptides, indicating that they are potentially exported proteins.[23] Indeed, we have shown that Bgp is a surface protein and its sequence analysis showed that the mature Bgp protein lacks the signal peptide.[23] Synthesis of MtnN and its cellular localization and enzymatic activity have not yet been determined. The cytoplasmic Pfs in the Lyme spirochaetes also exhibits MTA/SAH nucleosidase activity[24] and is a part of the four-gene (BB0374-*pfs-metK-luxS*) operon encoding proteins involved in the synthesis of the quorum-sensing molecule, AI-2. Lyme spirochaetes are the only known bacteria in which more than one copy of nucleosidase genes are present, with two gene products apparently exported.[25] The *B. burgdorferi* genome is rather small (1.52 Mb), and is approximately one-third of the size of the *Escherichia coli* genome (4.6 Mb). The presence of multiple MTA/SAH nucleosidases suggests that the enzymes are important for Lyme disease spirochaetes. Since *B. burgdorferi* lacks a majority of the biosynthetic pathways, MTA/SAH nucleosidases could play a critical role in the salvage of the purine adenine from MTA and SAH that is derived from both pathogen and host metabolisms. *B. burgdorferi* is likely to recycle this macromolecule building block more efficiently due to the presence of MTA/SAH nucleosidase enzymes both in the cytoplasm and on the spirochaete surface. Therefore, this enzyme offers us a unique opportunity to explore substrate analogues as antimicrobials against this important human pathogen.

The slow growth and unreliable colony formation ability of *B. burgdorferi* on solid media makes traditional plating methods unsuitable to screen and assess the effect of antimicrobials on spirochaete viability. Therefore, we have developed here a fluorescence-based high-throughput screening system involving a combination of Hoechst 33342 and Sytox Green nucleic acid stains to distinguish total and dead spirochaetes, respectively. Sytox Green is excluded by the plasma membrane of live organisms, and hence it stains nucleic acids of only the dead or physiologically compromised microbes.[26,27] A direct correlation was observed between Sytox Green staining and the proportion of dead spirochaetes in the sample. After comparing the activities of four MTA/SAH nucleosidase inhibitors on recombinant *B. burgdorferi* Bgp and Pfs proteins, we determined the effects of these compounds on spirochaete growth by employing this nucleic acid stain combination. Lastly, structure-based modelling was used to visualize potential interactions of MTA analogues with *B. burgdorferi* nucleosidases and to predict modifications that may lead to more selective and potent antiborrelial agents.

Materials and methods

Bacterial strains and culture

B. burgdorferi isolate B314, a high-passage, non-infectious derivative of the infectious B31 strain, which has lost all endogenous plasmids except cp26 and cp32, and an infectious strain N40 clone D10/E9 were used in this study. Since the lp28-4 plasmid possessing the *mtnN* gene is missing in B314, this isolate can only express Pfs and Bgp while the infectious N40 strain can possibly express all three genes, *pfs, bgp* and *mtnN*. The spirochaetes were grown at 33°C in BSK II medium containing 6% rabbit serum to a density of 10^8 spirochaetes/mL for each assay. To study the effect of inhibitors and ampicillin on the growth of *B. burgdorferi*, cultures were grown in a 5% CO_2 incubator at 37°C.

Assessment of the fluorescence-based system in high-throughput screening of live–dead B. burgdorferi

B. burgdorferi cultures were grown to a density of $\sim 10^8$ spirochaetes/mL and divided into two aliquots. One aliquot was incubated at 60°C for 30 min to kill the spirochaetes. A 10-fold serial dilution of dead *B. burgdorferi* was prepared in remaining live bacterial suspension such that the ratio of live spirochaetes decreased from 100% to 0% and dead spirochaetes increased from 0% to 100% (i.e. 100:0 to a final 0:100 ratio of live–dead *B. burgdorferi*). Two hundred microlitres of culture mixture was transferred to each

well of a 96-well black plate with a clear bottom (Catalog number 3603, Corning Incorporated, NY, USA). Two microlitres of a 1:1 mixture of 5 μM Sytox Green and 10 μM Hoechst 33342 was added to each well. After mixing, the plate was incubated at 37°C for 1–2 h and the Sytox Green (extinction 504 nm/emission 523 nm) and Hoechst 33342 (extinction 350 nm/emission 461 nm) fluorescences were measured using a Spectramax M2 spectrophotometer/microplate reader (Molecular Devices, CA, USA). The ratio of the fluorescence emission due to Sytox Green binding to nucleic acids determined the presence of dead spirochaetes and staining with Hoechst, which estimated both live and dead *B. burgdorferi* in the sample, provided the net fluorescence due to the dead spirochaetes. The standard curve between the known percentage of dead spirochaetes and net Sytox Green fluorescence for B314 and N40 strains was prepared to determine the sensitivity of detection of dead non-infectious versus infectious *B. burgdorferi* strains. Six replicates were used for each treatment and each experiment was repeated at least three times to confirm the reproducibility of the assay.

For fluorescence microscopy, the spirochaetes were centrifuged after incubation with the stain mixture, washed once with PBS and mounted in a 1:1 PBS/glycerol mixture. Sealing with nail polish limited the evaporation and prevented movement of the cover glasses. Differential interference contrast (DIC) provision in the Nikon 80i fluorescence microscope was used to observe total spirochaetes present in any field of view. DAPI (for Hoechst 33342 staining) and FITC (for Sytox Green staining) filters were used with ×100 magnification Apo-Plan TIRF objective to examine whether total spirochaetes observed by DIC are also visualized by Hoechst staining and whether physiologically compromised spirochaetes are detectable by Sytox Green staining.

Effect of ampicillin on B. burgdorferi growth

Lyme disease is treated with penicillin, tetracycline and cephalosporin classes of antibiotics.[1,2] Therefore, the efficacy of the fluorescence-based assay system was first assessed using ampicillin treatment of *B. burgdorferi*. Ten 2-fold dilutions of ampicillin were prepared starting from 200 μg/mL. Ten microlitres of each antibiotic dilution was added to 190 μL of *B. burgdorferi* culture in each of the six replicate wells of the 96-well black plate to obtain final concentrations of ampicillin from 10 to 0.0195 μg/well. After mixing for 5 min, the plate was incubated overnight at 37°C with 5% CO_2. The Sytox Green and Hoechst 33342 mixture was then added to each well, mixed, incubated for 1–2 h at 37°C and the fluorescence measured as described earlier. A standard prepared with known live–dead *B. burgdorferi* mixtures was used to calculate the percentage of dead/killed spirochaetes present in each treated sample.

Examination of substrate and inhibitor activity for B. burgdorferi MTA/SAH nucleosidases, Bgp and cytoplasmic Pfs

Unlike other bacteria, *B. burgdorferi* contains cytoplasmic (Pfs) and homologous cell surface proteins (Bgp and probably also MtnN), with at least Bgp and Pfs showing MTA/SAH nucleosidase activity.[24] For the present study, recombinant His-tagged Bgp and Pfs were expressed and purified as previously described.[24] The concentrations of recombinant Bgp and Pfs were determined using a Cary 100 scanning UV/Visible spectrophotometer (Varian, Palo Alto, CA, USA), and absorbance 280 (0.1%) values of 0.705 (Bgp) and 0.487 (Pfs). Enzyme activity was studied using a UV assay that follows the drop in absorbance at 275 nm that accompanies the conversion of the nucleoside into adenine and the corresponding thiosugar.[28,29] Specific activity measurements employed reaction mixtures containing 100 μM nucleoside and 100 mM sodium phosphate buffer at the optimized pH for each enzyme (pH 7 for Bgp; pH 5 for Pfs). Substrate nucleosides (MTA and SAH) and the inhibitor formycin A (FMA) were obtained from Sigma (St Louis, MO, USA). The inhibitors 5′-*p*-nitrophenylthioadenosine (*p*NO_2PhTA) and 5′-*p*-aminophenylthioadenosine (*p*NH_2PhTA) were gifts from Drs M. K. Riscoe and R. W. Winter (Veterans Affairs Medical Center, Portland, OR, USA). The transition-state analogue, BnT-DADMe-ImmA, was a gift from Drs Y. S. Babu and J. Zhang (BioCryst Pharmaceuticals, Birmingham, AL, USA). Conversion of substrate into adenine was calculated using an extinction coefficient (275 nm) for nucleoside decay of 1.6 $mM^{-1}cm^{-1}$. Concentrations of nucleosides were estimated by UV absorbance at 260 nm and an extinction coefficient of 15400 $M^{-1}cm^{-1}$. Reactions were initiated by the addition of 1–2 μg of enzyme and followed for 20–30 min at 22°C. For the determination of kinetic constants, substrates (MTA or SAH) were tested from 1 to 100 μM, with at least triplicate measurements performed at each concentration. Kinetics data were fitted to the Michaelis–Menten equation using Igor Pro 5.0 (Wavemetrics, Lake Oswego, OR, USA). Enzyme inhibition was analysed using the UV assay, with varying concentrations of the inhibitor (10–500 nM for BnT-DADMe-ImmA; 1–10 μM for *p*NO_2PhTA and *p*NH_2PhTA; and 25–250 μM for FMA) incorporated into reactions containing 100 μM MTA.[29] Controls having either no enzyme or no inhibitor were included in all experiments. The inhibition constant (K_i) was obtained by fitting the initial rate and inhibitor concentration to an equation for competitive inhibition:

$$V_0'/V_0 = (K_m + [S])/\{(K_m + [S] + K_m[I]/K_i)\}$$

where V_0' and V_0 are the initial rates of the inhibited and uninhibited reactions, respectively, [*I*] the inhibitor concentration and [*S*] the concentration of MTA.[29]

Assessment of the selected inhibitors of MTA/SAH nucleosidase as antimicrobials against B. burgdorferi

Four MTA/SAH nucleosidase inhibitors, FMA, *p*NO_2PhTA, *p*NH_2PhTA and BnT-DADMe-ImmA, were selected on the basis of the results of an *in vitro* assay with purified *B. burgdorferi* Bgp and Pfs proteins. Fivefold serial dilutions of each of the inhibitors were prepared from 200 to 0.32 μM (final concentrations of 10–0.016 μM). Four replicates of each treatment were used. The experiment was conducted as described earlier for ampicillin, and fluorometric and microscopic observations taken. To distinguish the bacteriostatic versus bactericidal activities of the inhibitors, the plate was incubated for 7 days. An aliquot of 2 μL of culture from each well was transferred to 1 mL of BSK II medium containing rabbit serum, to allow viable spirochaetes in the sample to recover and grow. After 14–21 days of incubation of culture tubes without inhibitors at 33°C, the presence of viable, motile spirochaetes was recorded using a dark-field microscope.

Modelling studies

High homology between *B. burgdorferi* MTA/SAH nucleosidase sequences and the corresponding *E. coli* enzyme (which has several solved crystal structures) and complete conservation of active site residues involved in catalysis were used in preliminary modelling studies to generate three-dimensional structures for Bgp and Pfs that might be instructive for future drug design. Initial models were

created using the structural coordinates for *E. coli* nucleosidase containing bound FMA (PDB accession no. 1NC3A). Sequence threading was accomplished using the program SWISS-Model and sequence overlays were further refined using ViewerPro 4.2 (Accelerys).[30–32]

Results

Sensitivity of detection of dead or dying B. burgdorferi by Sytox Green stain

Spirochaetes killed by heating at 60°C for 30 min were used to generate a standard curve between relative fluorescence (Sytox/Hoechst) and known percentage of dead/physiologically compromised *B. burgdorferi* cells. In this assay, the green fluorescence of *B. burgdorferi* isolate B314 (Figure 1a) showed a high co-efficient of correlation (r^2=0.962) with dead bacteria, indicating that staining of the nucleic acids by Sytox Green only occurs when viability of the spirochaetes is affected. Sensitivity of detection using Sytox Green stain was 10% dead spirochaetes since the assay could detect this level of killed *B. burgdorferi* reproducibly. The fluorescence values obtained using Hoechst 33342 DNA stain among different treatments within an experiment showed a standard deviation of <4% (data not shown). These results indicate that the total proportion of bacteria (live plus dead) in each sample, as detected by Hoechst staining, was accurately determined among different treatments, offering it to be a valuable control to assess consistency in spirochaete number in this assay system.

IC_{50} determination of ampicillin against B. burgdorferi using fluorescence-based assay system

Non-infectious *B. burgdorferi* isolate B314 was treated with 2-fold serial dilutions of ampicillin starting with 10 μg/200 μL of culture per well for 24 h. Determination of net Sytox Green fluorescence by fluorometric analysis indicated that similar to the heat-killed bacteria, *B. burgdorferi* were also unable to exclude this nucleic acid stain after treatment with ampicillin (Figure 1b). The IC_{50} of ampicillin calculated from the graphs (Figure 1a and b) was 0.35 μg per well or 1.75 μg/mL of B314 culture.

A similar analysis of the *B. burgdorferi* N40 strain (Figure 1c) showed that Sytox Green stain could distinguish dead and infectious spirochaetes as well. Again, a high

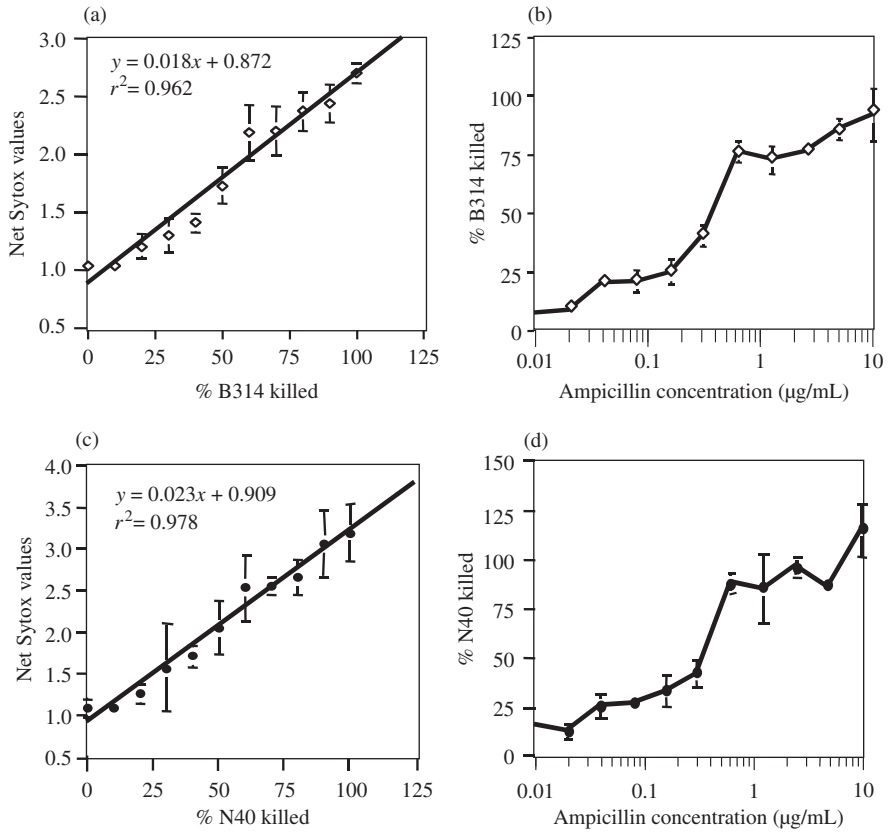

Figure 1. Sytox Green staining of both dead non-infectious *B. burgdorferi* isolate B314 and infectious *B. burgdorferi* strain N40 clone D10/E9 can be used to determine the IC_{50} of ampicillin by fluorometric analysis equally effectively. (a and c) Different dilutions of heat-killed (60°C for 30 min) B314 and N40 spirochaetes in the samples were examined after staining with Hoechst 33342/Sytox Green fluorescent DNA staining dyes. Quantification of Sytox Green (extinction 504 nm/emission 523 nm) fluorescence was normalized with the fluorescence obtained by Hoechst staining (extinction 350 nm/emission 461 nm) after measuring the fluorescence using a Spectramax M2 spectrophotometer/microplate reader. A standard curve prepared between net Sytox Green fluorescence and known dead spirochaetes showed a high coefficient of correlation (r^2=0.962 and 0.978 for B314 and N40, respectively). (b and d) The standard curve was used to determine the percentage killing of the B314 isolate after treatment with different concentrations of ampicillin overnight. The IC_{50} for the N40 strain (d) was the same (1.75 μg/mL) as that for the non-infectious isolate B314 (c).

coefficient of correlation (r^2=0.978) was observed between the known percentage of dead N40 spirochaetes present in a sample and net Sytox Green fluorescence values (Figure 1c). Furthermore, IC_{50} for ampicillin against N40 strain is equivalent to that for the B314 isolate, i.e. 1.75 μg/mL of culture (Figure 1b–d), indicating that this stain can detect dead non-infectious and infectious Lyme spirochaetes indistinguishably. Therefore, only the infectious N40 strain clone D10/E9 was used for all further experiments.

For further validation of our assay, we examined the spirochaetes using fluorescence microscopy. As predicted, all spirochaetes present in a field of view were visible by both DIC microscopy as well as by Hoechst staining (Figure 2). However, only spirochaetes treated with heat (60°C) showed bright green fluorescence using the FITC filter due to the nucleic acids staining with Sytox Green. Bleaching of the stains was very quick for *B. burgdorferi* treated with ampicillin, probably due to the beginning of DNA degradation, and was not suitable for photomicroscopy (data not shown).

Kinetic analysis of MTA/SAH nucleosidase substrate analogues with purified recombinant Bgp and Pfs proteins

Specific activity measurements performed at saturating levels of MTA or SAH confirmed that both Bgp and Pfs are dual-substrate-specific enzymes. Freshly prepared Bgp and Pfs exhibited specific activities for MTA of 4.1 and 4.4 U/mg enzyme and for SAH 3.1 and 3.7 U/mg, respectively (Table 1), indicating that each of the preparations contained similar levels of active enzyme. The nucleoside analogue, *p*NH_2PhTA, was a very poor substrate for Bgp (0.2 U/mg) and Pfs (0.024 U/mg), with no substrate activity detected at concentrations <50 μM (data not shown). The analogue *p*NO_2PhTA was a slightly better substrate for Pfs (2.0 U/mg) than for Bgp (0.83 U/mg), but here as well, detectible substrate activity <20 μM was unreliable. As expected, FMA and BnT-DADMe-ImmA were not cleaved due to the absence of a hydrolysable glycosidic linkage. A summary of the results of kinetic analysis of substrate and inhibitor activities is found in Figure 3. For the two enzymes, only the differences in activity against MTA and FMA were statistically significant ($P<0.01$; Student's *t*-test). The differences in activity between the two enzymes towards SAH, *p*NO_2PhTA, *p*NH_2PhTA and BnT-DADMe-ImmA were not significant ($P>0.05$), suggesting that each enzyme recognizes bulkier 5′ substitutions in compounds to similar levels. Of the inhibitors tested, BnT-DADMe-ImmA (K_i=2.3–3.4 nM) showed the tightest binding to the nucleosidases with K_i values roughly two to three orders of magnitude smaller than the Michaelis constant (K_m) values reported for MTA (K_m=0.7–5 μM) and SAH (K_m=1.2–1.6 μM). This result is expected, since BnT-DADMe-ImmA is a transition-state analogue, and belongs to a class of compounds that have previously been reported to show picomolar and femtomolar dissociation constants for the *E. coli* nucleosidase.[29]

With the exception of FMA, where the K_i (1.05 and 2.69 μM) was less than the 10 μM reported for the *E. coli* enzyme,[10] the inhibitors generally showed somewhat less activity towards the spirochaetal enzymes. For the late transition-state analogue BnT-DADMe-ImmA, the K_i value is substantially higher for Bgp (2.3 nM) and Pfs (3.4 nM) than that reported for *E. coli* nucleosidase (28 pM),[29] although it is similar to that reported for the *Streptococcus pneumoniae* enzyme (5 nM).[20]

High-throughput screening of different inhibitors of MTA/SAH nucleosidase on the growth of B. burgdorferi

Based upon the kinetic analysis with purified recombinant Bgp and Pfs of *B. burgdorferi* (Figure 3), we assessed the inhibitory activities of all four compounds against the infectious spirochaete

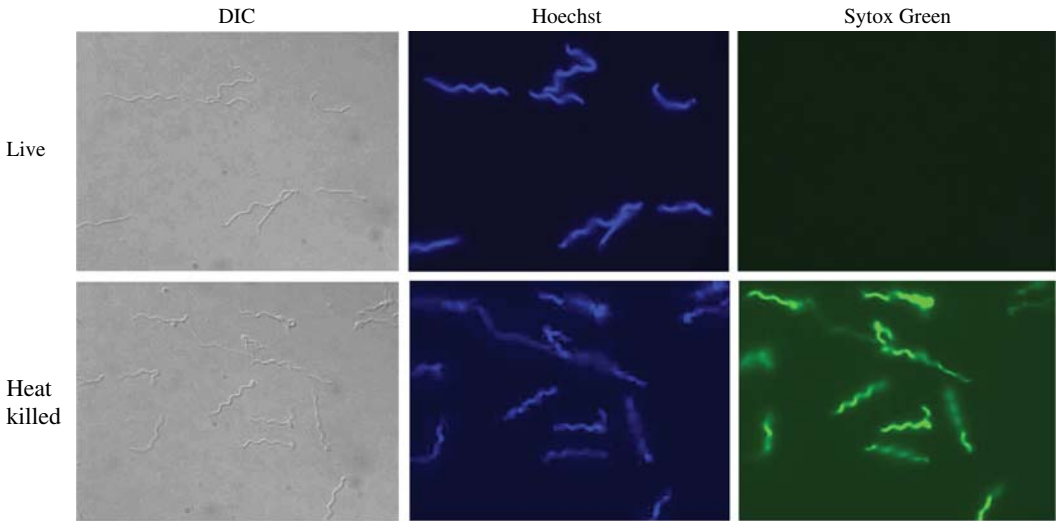

Figure 2. Microscopic examination of live and heat-killed *B. burgdorferi* strain N40 clone D10/E9 after Hoechst/Sytox Green double staining. The samples were centrifuged after incubation with the nucleic acid dyes, washed once with PBS and mounted in 1:1 PBS/glycerol mixture. The cover glasses were sealed with nail polish to limit evaporation. DIC provision in the Nikon 80i fluorescence microscope was used to observe total spirochaetes present in any field of view. DAPI (for Hoechst 33342 staining) and FITC (for Sytox Green) filters were used. Total spirochaetes were observed by Hoechst staining and physiologically compromised spirochaetes by Sytox Green staining by using an Apo-Plan TIRF ×100 magnification objective. This figure appears in colour in the online version of *JAC* and in black and white in the print version of *JAC*.

strain N40. The Hoechst/Sytox Green stain mixture was used to evaluate total and physiologically compromised *B. burgdorferi*, respectively. Calculation of the net Sytox Green fluorescence values (Sytox Green/Hoechst) after treatment with the inhibitors was followed by the determination of the bacteriostatic/dead bacteria present in the samples using the standard in Figure 1(c) to evaluate the inhibitory activities of these compounds. The results obtained with *p*NH_2PhTA and BnT-DADMe-ImmA indicate that even at a relatively high concentration (10 μM), these inhibitors only partially affected the physiological status of the spirochaetes (Figure 4). However, the fluorometric assay suggested that both *p*NO_2PhTA and FMA are highly effective inhibitors against *B. burgdorferi*. The MIC of these two inhibitors is lower than the least concentration tested here (0.016 μM) as detected by fluorometric analysis (Figure 4).

The effectiveness of this fluorometric assay system and potency of these inhibitors were further confirmed by microscopic examination of the samples. Indeed, microscopic examination after treatment confirmed the presence of dead or dying spirochaetes, as stained by Sytox Green (Figure 5). The staining

Table 1. Summary of specific activity measurements for Bgp and Pfs

Enzyme	Compound	Specific activity (U/mg)	Relative activity (%)
Bgp	MTA	4.1	100
	SAH	3.1	76
	pNH_2PhTA	0.2	5
	pNO_2PhTA	0.82	20
	FMA	0	0
	BnT-DADMe-ImmA	0	0
Pfs	MTA	4.4	100
	SAH	3.7	84
	pNH_2PhTA	0.024	0.6
	pNO_2PhTA	2.0	45
	FMA	0	0
	BnT-DADMe-ImmA	0	0

Enzyme activities were tested using the UV spectrophotometric assay (275 nm) and either 100 μM substrate (MTA and SAH) or 100 μM substrate analogue (*p*NH_2PhTA, *p*NO_2PhTA, FMA and BnT-DADMe-ImmA).

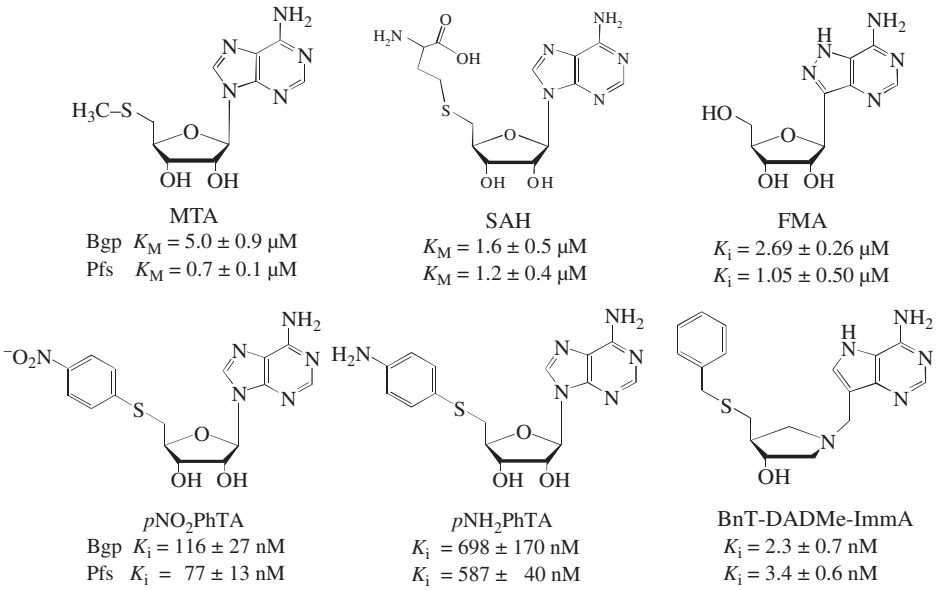

Figure 3. Summary of inhibition constants for MTA analogues compared with K_m values for native MTA and SAH substrates for Bgp and Pfs enzymes. Enzyme assays were conducted using UV spectrophotometry (275 nm) and pH conditions optimized for Bgp (pH 7) and Pfs (pH 5). For MTA and SAH, concentrations from 1 to 100 μM were evaluated. Inhibitor effects were determined using varying concentrations of inhibitor and a fixed concentration of MTA (100 μM). Inhibition constants were determined by fitting the initial rates of the inhibited (V_0') and uninhibited (V_0) reactions to the equation for competitive inhibition: $V_0'/V_0 = (K_m + [S])/\{(K_m + [S] + K_m[I]/K_i)\}$.[29] Inhibitor effects appear to be similar for each of the enzymes, with the strongest inhibition exhibited by the non-hydrolysable late transition-state analogue BnT-DADMe-ImmA (K_i=2.3 and 3.4 nM for BGP and Pfs, respectively).

was not as intense and uniform for the spirochaetes as observed by Sytox Green staining of the heat-killed spirochetes (Figure 2). However, fewer spirochaetes treated with pNH$_2$PhTA and BnT-DADMe-ImmA (average of $43.8 \pm 4.0\%$ and $45.1 \pm 3.1\%$, respectively, from 10 different fields) were visualized by Sytox Green staining when compared with those detected by Hoechst staining or DIC microscopy, while most spirochaetes stained with Sytox Green (average of $68.6 \pm 4.2\%$ from 10 fields) after treatment with pNO$_2$PhTA, complementing our results from fluorometric analysis. Exclusion of Sytox Green by several spirochaetes after FMA treatment (only an average of $51.3 \pm 5.5\%$ stained with Sytox Green) was surprising. Hence, pNO$_2$PhTA appears to be most effective against *B. burgdorferi* also by microscopic examination.

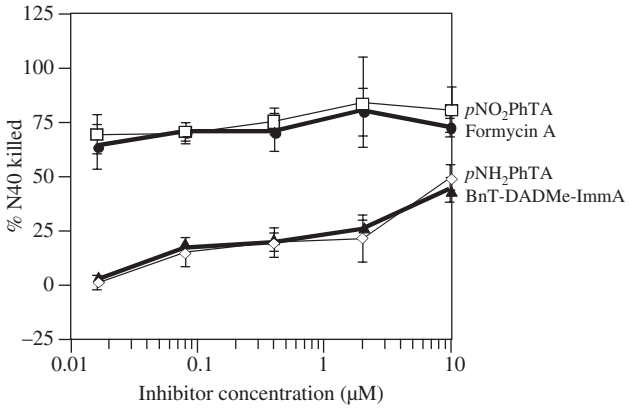

Figure 4. Treatment of *B. burgdorferi* with MTA/SAH nucleosidase inhibitors affects their membrane permeability. Fluorometric analysis of *B. burgdorferi* after treatment with four inhibitors overnight followed by staining with a Hoechst/Sytox Green mixture was conducted as described in the legend to Figure 1. Both pNO$_2$PhTA and FMA affected the physiological state of the spirochaetes significantly, as indicated by membrane permeability to Sytox Green, even at a concentration of 0.016 μM, while pNH$_2$PhTA and BnT-DADMe-ImmA showed much weaker antibacterial activities.

MTA/SAH substrate analogues show either bacteriostatic or bactericidal activities against infectious B. burgdorferi N40 strain

To examine whether the inhibitory activities of the four substrate analogues against spirochaetes have bactericidal or bacteriostatic effects, we recovered small aliquots (2 μL) from the treated samples daily and cultured *B. burgdorferi* in BSK II medium containing 6% rabbit serum without inhibitors. After treatment with all four compounds up to 4 days, at least some spirochaetes survived even after exposure to 10 μM (data not shown). However, we were unable to recover live spirochaetes when the N40 strain was treated with a higher concentration of FMA for 7 days. The recovery of spirochaetes was also poor after treatment with pNH$_2$PhTA. Such a subtle distinction between the three inhibitors was not possible with the fluorometric analysis. In these studies, FMA appears to be bactericidal against *B. burgdorferi* after prolonged treatment while the other three MTA nucleosidase inhibitors could be bacteriostatic under the tested concentrations.

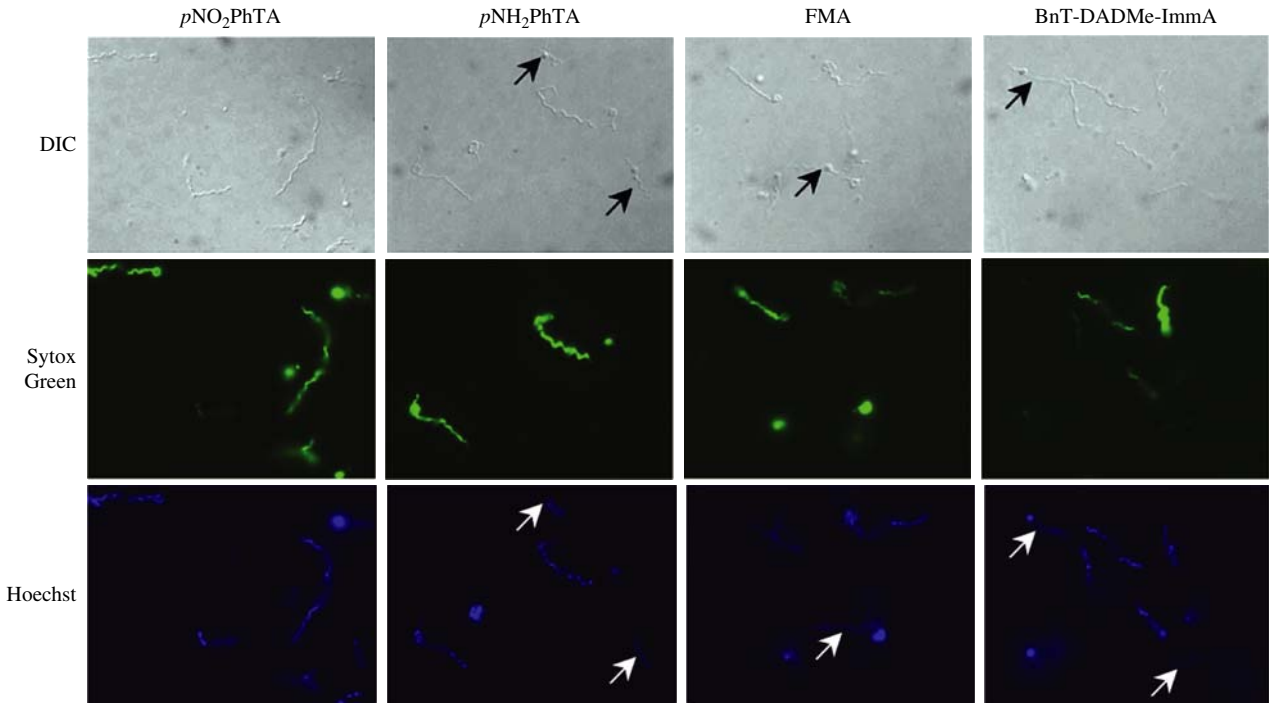

Figure 5. Microscopic examination of *B. burgdorferi* confirmed the adverse effects of MTA/SAH inhibitors on the physiological status of the spirochaetes. Almost all spirochaetes showed green fluorescence due to staining with Sytox Green after treatment with pNO$_2$PhTA, while several *B. burgdorferi* excluded this stain after NH$_2$PhTA and BnT-DADMe-ImmA treatment for 7 days (as marked by arrows), hence confirming our results with fluorometric analysis. Exclusion of Sytox Green by some *B. burgdorferi* after FMA treatment was unexpected. The presence of vesicular, cyst-like structures observed after each treatment indicated the damaging effect of all four inhibitors on the Lyme spirochaetes. This figure appears in colour in the online version of *JAC* and in black and white in the print version of *JAC*.

Modelling studies of Bgp and Pfs with FMA

The availability of a crystal structure of the *E. coli* MTA/SAH nucleosidase[33] with FMA bound in the active site allowed preliminary predictions of the three-dimensional features of Bgp and Pfs to be made using modelling programs (Figure 6a). Ribbon threading of the *B. burgdorferi* Pfs (in blue) onto the known *E. coli* enzyme structure (in yellow) predicts very similar structures without additional energy minimizations. Threading the Bgp enzyme (in pink) onto the *E. coli* enzyme also predicted highly similar structures, although a less organized loop structure was suggested in the model to replace regions of alpha helices found in Pfs. Surface charges and the orientation of the 5′-hydroxyl group (O5 in Figure 6b) facing out of the active site pocket supports the availability of the 5′ position of the nucleoside for modification. From the model, the purine-binding pocket is predicted to be more restricted in Pfs than Bgp.

Active site residues involved in catalysis (E12, E174 and D197) are strictly conserved in Bgp (E34, E209 and D232) and Pfs (E11, E181 and D204). As expected, the highly homologous cytoplasmic *E. coli* nucleosidase and Pfs are suggested to have essentially the same secondary and tertiary structure in the model. Of note, the Bgp backbone is predicted to loop away from the other two strands at a juncture between β8 and α4 (yellow arrow in front view) in a region that provides a face for the purine-binding site. As shown in Figure 6(b), modelling of the electrostatic surface charges suggests that this divergence has the effect of orienting the phenyl ring of F187 in Bgp outward from the active site. By comparison, F158 of Pfs (F151 in *E. coli*) shields the active site and forms stabilizing aromatic interactions with the adenine ring of the substrate.[13,20] Other small changes in the identity and position of residues around the entrance to the active site of Bgp are suggested as well in Figure 6(b). A replacement of Pfs F215 (*E. coli* F207) with slightly rotated Y243 in Bgp would predict a decrease in apparent shielding of N7 of the purine ring, while a substitution of Pfs I53 (I50 in *E. coli*) with V79 in Bgp suggests an increase in the accessibility of the bottom of the pocket.

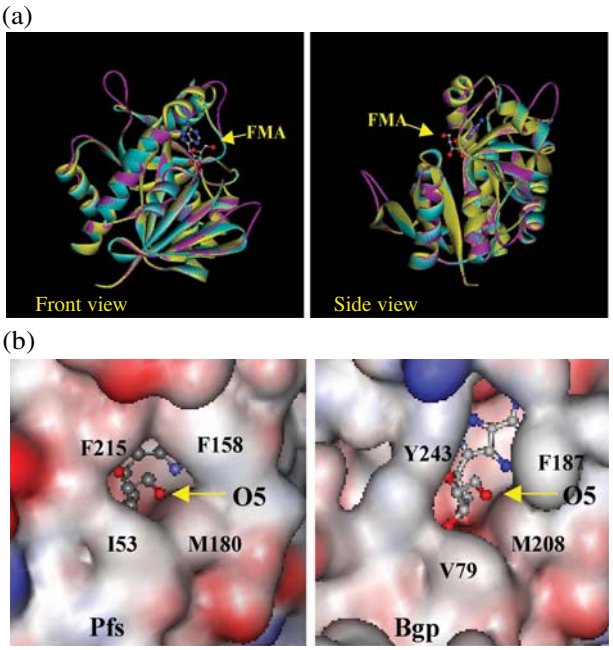

Figure 6. Superimposed ribbon structures of MTA/SAH nucleosidases and close-up of surface electrostatic maps of Bgp and Pfs enzyme active sites containing FMA. (a) The sequences of Bgp (pink) and Pfs (blue) were threaded onto the known three-dimensional structure of *E. coli* MTA/SAH nucleosidase monomer (PDB 1nc3A) (yellow) using SWISS-Model. A ball and stick structure of docked FMA is shown (blue=nitrogen; red=oxygen). Overall, the structures of Bgp and Pfs appear to be highly conserved with the *E. coli* enzyme. (b) In the close-up of the surface structural map of the MTA/SAH nucleosidases, charges are represented in red (negative) and blue (positive). The orientation of the 5′-hydroxyl group (O5 in the figure) facing out of the active site pocket supports the availability of the 5′ position of the nucleoside for modification. From the model, the purine-binding pocket is suggested to be more restricted in Pfs than Bgp. This figure appears in colour in the online version of *JAC* and in black and white in the print version of *JAC*.

Discussion

Limiting factors for the treatment of patients to curtail certain bacterial diseases are the incessant emergence of antibiotic resistance among various pathogens and intolerance of some patients against certain antibiotics.[2,34] These often lead to the employment of a combination regimen of drugs for treatment. Alternatively, relatively less effective drugs are included in the treatment of drug-intolerant patients. Therefore, there is an urgent need to explore novel physiological inhibitors as the potential antimicrobials against bacterial pathogens, including *B. burgdorferi*. Success of the enzymatic inhibitors as antimicrobials depends on: (i) their ability to selectively restrict the growth of the pathogens without interfering with the human enzymes; and (ii) their broad effectiveness against various pathogens. In this study, we have examined substrate analogues of MTA/SAH nucleosidase enzymes of *B. burgdorferi* as potential antimicrobials.

Two activities of nucleosidase, cleavage of MTA and SAH, are carried out by two different enzymes in mammals, MTA phosphorylase and SAH hydrolase.[35] While mammalian SAH hydrolase and bacterial MTA/SAH nucleosidase are not structurally similar, the crystal structures of the mammalian MTA phosphorylase enzyme and MTA/SAH nucleosidase of *E. coli* show significant similarities. A comparison of their active sites shows remarkable similarities in the residues involved in adenine binding, although the pocket enclosing N5 appears to be more open in the mammalian enzyme.[13] Significant structural differences exist in the ribose-binding site between the two enzymes, where phosphate-binding amino acid residues in MTA phosphorylase, Arg and Thr, are replaced by Ser and Gly in the bacterial nucleosidase, hence preventing the charge–charge interactions.[13,14] Importantly, the channel containing the 5′-alkylthio group of the MTA/SAH nucleosidase appears more open than in the mammalian enzyme, thus providing an explanation for the dual substrate specificity of the bacterial enzyme. Interactions between residues from the second chain of the nucleosidase dimer and the extended 5′-alkylthio group of SAH may provide additional stabilization and recognition.[15]

The models of *B. burgdorferi* proteins, while suggestive, should not be overinterpreted in the absence of true crystallographic evidence. The differences seen between the K_m values for MTA between Bgp (5 μM) and Pfs (0.7 μM) may be explained by the small structural differences suggested in the

models. These activity differences could also represent differences in the behaviours of the recombinant enzymes and conditions under which the assays were conducted. Prior evidence[24] supported a lower Bgp K_m for MTA (1.2 μM), which was more in line with the submicromolar values found for Pfs and the *E. coli* nucleosidase, but that assay followed the conversion of radioactive MTA into MTR, rather than direct spectrophotometric observance of substrate conversion that is reported here. In either case, the K_m values reported here for both enzymes for MTA and SAH are similar to the values in the literature for the *E. coli* and *Klebsiella* nucleosidases[28,36,37] and roughly an order of magnitude lower than those recently reported for *S. pneumoniae* nucleosidase.[20]

Taking advantage of the suggested structural similarities of MTA/SAH nucleosidases, we first conducted kinetic analysis of four previously examined inhibitors,[13,15,36,38,39] with the purified recombinant Bgp and Pfs proteins followed by their evaluation with intact *B. burgdorferi*. Fluorometric analysis of the effect of MTA/SAH nucleosidase inhibitors on *B. burgdorferi* facilitated the identification of *p*NO_2PhTA and FMA as more effective compounds against the spirochaetes. Interestingly, the IC_{50} of these inhibitors in damaging the plasma membrane integrity is much lower than that reported for the purified *E. coli* enzyme previously[36,40] as well as shown here (Figure 3) for purified *B. burgdorferi* nucleosidases. These results suggest that MTA/SAH nucleosidase could be an even better target of the substrate analogues as antimicrobials in *B. burgdorferi* than other bacterial pathogens. This is likely due to the additive effect of these inhibitors on all three spirochaete enzymes in the intact organisms. In addition, *B. burgdorferi* may be more permeable to these inhibitors when compared with Gram-negative bacteria since their outer membrane lacks lipopolysaccharide and is more flexible. FMA showed a significant bactericidal activity against *B. burgdorferi* after prolonged treatment. Interestingly, *p*NH_2PhTA, and not *p*NO_2PhTA, seems to result in a significant level of killing of the spirochaetes at high dose (10 μM) on prolonged treatment, as detected by cultivation in the absence of an inhibitor. Such a subtle distinction between the inhibitors' activities was not possible with the fluorometric, and even microscopic, analysis. In a human bone marrow cell growth assay, both *p*NH_2PhTA and *p*NO_2PhTA showed low toxicity, with IC_{50} values >100 μM (K. A. C., unpublished data), suggesting that their toxicity to *B. burgdorferi* is selective.

In summary, we have developed a novel high-throughput, fluorometric screening method for *B. burgdorferi* viability after treatment with the potential antimicrobials, and have assessed its effectiveness using MTA/SAH nucleosidase as a target. After characterization of the inhibitors in our collection using purified recombinant *B. burgdorferi* nucleosidase, we further used this fluorometric method, as well as analysis by microscopy and culture to assess the potency of these inhibitors as antimicrobials. We report here that *p*NO_2PhTA and FMA have high inhibitory activities on *B. burgdorferi* even at very low concentrations (0.016 μM). In addition, FMA is potentially bactericidal when treatment is extended to 7 days. These results indicate that the MTA/SAH nucleosidase enzyme is an excellent target for the discovery of new antimicrobials against Lyme disease spirochaetes. This study further supports potential use of novel inhibitors against this critically important enzyme for the treatment of Lyme disease in the future, especially when patients are intolerant to doxycycline, amoxicillin or cefuroxime axetil, for pregnant women or potentially for patients suffering from chronic Lyme disease. We will examine other substrate analogues for this enzyme as well as attempt chemical modification of already effective inhibitors based upon the structure and residues of the substrate-binding site of the enzymes to further enhance their bactericidal activity against Lyme disease spirochaetes in the future.

Acknowledgements

We thank Karl Drlica for careful review of the manuscript prior to submission.

Funding

This work was supported by a pilot grant from the National Research Fund for Tick-borne Diseases and a chapter grant (New Jersey) from the Arthritis Foundation to N. P., and the Idaho IDeA programme (NIH P20RR016454), a pilot grant from the Mountain States Tumor and Medical Research Institute (MSTMRI) and the Boise State University Faculty Research programme to K. A. C.

J. A. M. was supported by an undergraduate premedical research fellowship from MSTMRI.

Transparency declarations

None to declare.

All studies involving Lyme spirochaetes were conducted by N. P. and her student S. P., and all kinetic analyses were carried out by K. A. C. and J. A. M. (his student). K. A. C. also conducted structural modelling of *B. burgdorferi* enzymes. N. P. and K. A. C. wrote the article.

References

1. Wormser GP, Dattwyler RJ, Shapiro ED *et al.* Single-dose prophylaxis against Lyme disease. *Lancet Infect Dis* 2007; **7**: 371–3.

2. Wormser GP, Dattwyler RJ, Shapiro ED *et al.* The clinical assessment, treatment, and prevention of Lyme disease, human granulocytic anaplasmosis, and babesiosis: clinical practice guidelines by the Infectious Diseases Society of America. *Clin Infect Dis* 2006; **43**: 1089–134.

3. Jackson CR, Boylan JA, Frye JG *et al.* Evidence of a conjugal erythromycin resistance element in the Lyme disease spirochete *Borrelia burgdorferi*. *Int J Antimicrob Agents* 2007; **30**: 496–504.

4. Sufrin JR, Meshnick SR, Spiess AJ *et al.* Methionine recycling pathways and antimalarial drug design. *Antimicrob Agents Chemother* 1995; **39**: 2511–5.

5. Duerre JA. A hydrolytic nucleosidase acting on *S*-adenosylhomocysteine and on 5′-methylthioadenosine. *J Biol Chem* 1962; **237**: 3737–41.

6. Chen X, Schauder S, Potier N *et al.* Structural identification of a bacterial quorum-sensing signal containing boron. *Nature* 2002; **415**: 545–9.

7. Schauder S, Bassler BL. The languages of bacteria. *Genes Dev* 2001; **15**: 1468–80.

8. Winzer K, Hardie KR, Williams P. Bacterial cell-to-cell communication: sorry, can't talk now—gone to lunch! *Curr Opin Microbiol* 2002; **5**: 216–22.

9. Gianotti AJ, Tower PA, Sheley JH *et al*. Selective killing of *Klebsiella pneumoniae* by 5-trifluoromethylthioribose. Chemotherapeutic exploitation of the enzyme 5-methylthioribose kinase. *J Biol Chem* 1990; **265**: 831–7.

10. Singh V, Lee JE, Nunez S *et al*. Transition state structure of 5′-methylthioadenosine/*S*-adenosylhomocysteine nucleosidase from *Escherichia coli* and its similarity to transition state analogues. *Biochemistry* 2005; **44**: 11647–59.

11. Li X, Chu S, Feher VA *et al*. Structure-based design, synthesis, and antimicrobial activity of indazole-derived SAH/MTA nucleosidase inhibitors. *J Med Chem* 2003; **46**: 5663–73.

12. Schramm VL, Gutierrez JA, Cordovano G *et al*. Transition state analogues in quorum sensing and SAM recycling. *Nucleic Acids Symp Ser (Oxf)* 2008; **52**: 75–6.

13. Lee JE, Settembre EC, Cornell KA *et al*. Structural comparison of MTA phosphorylase and MTA/AdoHcy nucleosidase explains substrate preferences and identifies regions exploitable for inhibitor design. *Biochemistry* 2004; **43**: 5159–69.

14. Lee JE, Cornell KA, Riscoe MK *et al*. Structure of *E. coli* 5′-methylthioadenosine/*S*-adenosylhomocysteine nucleosidase reveals similarity to the purine nucleoside phosphorylases. *Structure (Camb)* 2001; **9**: 941–53.

15. Lee JE, Singh V, Evans GB *et al*. Structural rationale for the affinity of pico- and femtomolar transition state analogues of *Escherichia coli* 5′-methylthioadenosine/*S*-adenosylhomocysteine nucleosidase. *J Biol Chem* 2005; **280**: 18274–82.

16. Pajula RL, Raina A. Methylthioadenosine, a potent inhibitor of spermine synthase from bovine brain. *FEBS Lett* 1979; **99**: 343–5.

17. Raina A, Tuomi K, Pajula RL. Inhibition of the synthesis of polyamines and macromolecules by 5′-methylthioadenosine and 5′-alkylthiotubercidins in BHK21 cells. *Biochem J* 1982; **204**: 697–703.

18. Borchardt RT, Creveling CR, Ueland PM. *Biological Methylation and Drug Design*. Clifton, NJ: Humana Press, 1986.

19. von Lackum K, Babb K, Riley SP *et al*. Functionality of *Borrelia burgdorferi* LuxS: the Lyme disease spirochete produces and responds to the pheromone autoinducer-2 and lacks a complete activated-methyl cycle. *Int J Med Microbiol* 2006; **296** Suppl 40: 92–102.

20. Singh V, Shi W, Almo SC *et al*. Structure and inhibition of a quorum sensing target from *Streptococcus pneumoniae*. *Biochemistry* 2006; **45**: 12929–41.

21. Babb K, von Lackum K, Wattier RL *et al*. Synthesis of autoinducer 2 by the Lyme disease spirochete, *Borrelia burgdorferi*. *J Bacteriol* 2005; **187**: 3079–87.

22. Riley SP, Bykowski T, Babb K *et al*. Genetic and physiological characterization of the *Borrelia burgdorferi* ORF BB0374-*pfs-metK-luxS* operon. *Microbiology* 2007; **153**: 2304–11.

23. Parveen N, Leong JM. Identification of a candidate glycosaminoglycan-binding adhesin of the Lyme disease spirochete *Borrelia burgdorferi*. *Mol Microbiol* 2000; **35**: 1220–34.

24. Parveen N, Cornell KA, Bono JL *et al*. Bgp, a secreted GAG-binding protein of *B. burgdorferi* strain N40, displays nucleosidase activity and is not essential for infection of immunodeficient mice. *Infect Immun* 2006; **74**: 3016–20.

25. Fraser CM, Casjens S, Huang WM *et al*. Genomic sequence of a Lyme disease spirochaete *Borrelia burgdorferi*. *Nature* 1997; **390**: 580–6.

26. Roth BL, Poot M, Yue ST *et al*. Bacterial viability and antibiotic susceptibility testing with SYTOX green nucleic acid stain. *Appl Environ Microbiol* 1997; **63**: 2421–31.

27. Langsrud S, Sundheim G. Flow cytometry for rapid assessment of viability after exposure to a quaternary ammonium compound. *J Appl Bacteriol* 1996; **81**: 411–8.

28. Singh V, Shi W, Evans GB *et al*. Picomolar transition state analogue inhibitors of human 5′-methylthioadenosine phosphorylase and X-ray structure with MT-immucillin-A. *Biochemistry* 2004; **43**: 9–18.

29. Singh V, Evans GB, Lenz DH *et al*. Femtomolar transition state analogue inhibitors of 5′-methylthioadenosine/*S*-adenosylhomocysteine nucleosidase from *Escherichia coli*. *J Biol Chem* 2005; **280**: 18265–73.

30. Schwede T, Kopp J, Guex N *et al*. SWISS-MODEL: an automated protein homology-modeling server. *Nucleic Acids Res* 2003; **31**: 3381–5.

31. Arnold K, Bordoli L, Kopp J *et al*. The SWISS-MODEL workspace: a web-based environment for protein structure homology modelling. *Bioinformatics* 2006; **22**: 195–201.

32. Kopp J, Schwede T. The SWISS-MODEL repository of annotated three-dimensional protein structure homology models. *Nucleic Acids Res* 2004; **32**: D230–4.

33. Lee JE, Cornell KA, Riscoe MK *et al*. Expression, purification, crystallization and preliminary X-ray analysis of *Escherichia coli* 5′-methylthioadenosine/*S*-adenosylhomocysteine nucleosidase. *Acta Crystallogr D Biol Crystallogr* 2001; **57**: 150–2.

34. Montgomery RR, Schreck K, Wang X *et al*. Human neutrophil calprotectin reduces the susceptibility of *Borrelia burgdorferi* to penicillin. *Infect Immun* 2006; **74**: 2468–72.

35. Riscoe MK, Ferro AJ, Fitchen JH. Methionine recycling as a target for antiprotozoal drug development. *Parasitol Today* 1989; **5**: 330–3.

36. Cornell KA, Swarts WE, Barry RD *et al*. Characterization of recombinant *Escherichia coli* 5′-methylthioadenosine/*S*-adenosylhomocysteine nucleosidase: analysis of enzymatic activity and substrate specificity. *Biochem Biophys Res Commun* 1996; **228**: 724–32.

37. Cornell KA, Winter RW, Tower PA *et al*. Affinity purification of 5-methylthioribose kinase and 5-methylthioadenosine/*S*-adenosylhomocysteine nucleosidase from *Klebsiella pneumoniae*. *Biochem J* 1996; **317**: 285–90.

38. Lee JE, Smith GD, Horvatin C *et al*. Structural snapshots of MTA/AdoHcy nucleosidase along the reaction coordinate provide insights into enzyme and nucleoside flexibility during catalysis. *J Mol Biol* 2005; **352**: 559–74.

39. Siu KK, Lee JE, Smith GD *et al*. Structure of *Staphylococcus aureus* 5′-methylthioadenosine/*S*-adenosylhomocysteine nucleosidase. *Acta Crystallogr Sect F Struct Biol Cryst Commun* 2008; **64**: 343–50.

40. Lee JE, Cornell KA, Riscoe MK *et al*. Structure of *Escherichia coli* 5′-methylthioadenosine/*S*-adenosylhomocysteine nucleosidase inhibitor complexes provide insight into the conformational changes required for substrate binding and catalysis. *J Biol Chem* 2003; **278**: 8761–70.